Manipulating Thermal Conductance of Supported Graphene via Surface Hydroxylation of Substrates

Liu Cui [1, 2, *], Sanqiang Shi [2], Zhao Li [1], Gaosheng Wei [1], Xiaoze Du [1, *]

[1] *Key Laboratory of Condition Monitoring and Control for Power Plant Equipment, Ministry of Education, North China Electric Power University, Changping, Beijing 102206, China*

[2] *Department of Mechanical Engineering, The Hong Kong Polytechnic University, Hung Hom, Kowloon, Hong Kong, China*

[*]To whom correspondence should be addressed.

E-mail: liucui@ncepu.edu.cn (L. Cui); duxz@ncepu.edu.cn (X. Du)

Abstract

Surface functionalization of substrates is a promising strategy to tune the thermal transport in supported graphene. In this work, we have conducted molecular dynamics simulations to investigate how the surface hydroxylation of amorphous SiO_2 substrate affects the heat conduction in supported graphene. The results show that the thermal conductivity of supported graphene is decreased by introducing hydroxyl groups on the substrate surface. The underlying physics of thermal conductivity suppression is explained by analyzing the phonon spectral energy density, lifetime and participation ratio. We have observed that the surface hydroxylation decreases the phonon lifetime and causes the remarkable damping of ZA phonons. Moreover, the hydroxyl groups induce modifications of graphene configuration, which results in the phonon localization and correspondingly the low thermal conductivity. Our findings highlight the importance of substrate surface on thermal conductivity of supported graphene, and provide guidance on the design of substrates to control the heat transport in graphene.

1. Introduction

Graphene is a single atomic layer of graphite and defined as a one-atom-thick planar sheet of carbon atoms densely packed in a honeycomb lattice [1]. It has showed great potential to be used as a thermal management material for electronic nanodevices [2], owing to its ultrahigh thermal conductivity (ranging from 1500-5300 W/(m·K) [3-6]). In most electronic nanodevices, however, graphene is supported on a medium instead of being suspended [7]. Understanding the effect of supporting medium on thermal properties is not only scientifically but also technologically important to optimize the performance and reliability of graphene-based devices.

The in-plane heat transfer in supported graphene has raised considerable interest [8]. Recent investigations have concluded that the thermal conductivity of graphene undergoes severe degradation, when graphene is supported on a copper substrate [9], a SiC substrate [10], an amorphous SiO_2 substrate [11-14] or a residual polymeric layer [15]. In general, it is thought that the degradation of remarkable thermal conductivity of graphene is attributed to the damping of out-of-plane flexural (ZA) phonons, which is related to the graphene-substrate interaction [13-14]. However, it is still an open question whether increasing the graphene-substrate strength enhances [13] or reduces [12, 14] heat transfer of graphene.

For applications of graphene in electronic devices, amorphous SiO_2 is one of the most common substrates [11, 16], due to its insulating properties and its easy integration in silicon based electronics. It has been reported that the surface of amorphous silica exhibits various features (e.g. hydroxylation and reconstruction) [17-18]. The surface structure may affect the van der Waals (vdW) interaction between the graphene and substrate. Meanwhile, it is associated with the surface roughness of substrate, which results in the change of graphene configuration. It has been found that the surface

modifications of amorphous SiO_2 substrates could induce variations in thermal properties of graphene on them. Lee et al. [19] reported that the thermal conductivity of supported graphene is sensitive to both the amorphous SiO_2 substrate-surface roughness and graphene conformity with modulation within 500 W/(m·K). France-Lanord et al. [20] recently showed the surface hydroxylation of amorphous SiO_2 substrate diminishes the single-phonon contribution to the graphene thermal conductivity but helps in preserving the collective phonon excitations in graphene. To date, however, the understanding of substrate surface engineering for the manipulation of graphene thermal conductance is still lacking. The underlying physical mechanisms in view of the spectral phonon information need to be further investigated.

In this paper, the influence of surface hydroxylated substrate on the thermal transport in graphene was studied by molecular dynamics (MD) simulations. The results demonstrate that the thermal conductivity of supported graphene can be decreased by introducing hydroxyl groups on the surface of amorphous silica substrate. The physical insights for the reduced thermal conductance were gained by analyzing the phonon spectral energy density, lifetime and participation ratio.

2. Model and methodology

The models of supported graphene sheets are shown in Fig. 1a and 1b. The bulk amorphous SiO_2 substrate was generated by heating α-quartz SiO_2 up to 6000 K and then cooling it down to the desired temperatures at a constant cooling rate of 10^{13} K/s. This approach has been widely used to simulate amorphous SiO_2 in previous literatures [12, 14, 21]. To create the SiO_2 surface from the amorphous structure, a void was added in the *z*-direction. Some Si and O atoms on the SiO_2 surface are not fully coordinated. It should be noted that covalent bonds cannot break or form during our MD simulations.

Therefore, these Si and O atoms at the surface remain uncoordinated. The covalent bonds cannot form between the graphene and SiO_2 substrate, which may have a great effect on thermal conductivity of supported graphene. In this paper, the results for supported graphene are obtained under the assumption that the interaction between graphene and substrate is a vdW interaction. The dimensions of the amorphous SiO_2 substrate are 10, 5, 2.2 nm in length (*x*-direction), width (*y*-direction), and thickness (*z*-direction), respectively. The substrates with similar thickness have also been applied to electronic [22] and thermal [14] simulations. To create the hydroxylated substrate, an amorphous SiO_2 slab with dimensions of 10×5×3.2 nm (length×width×thickness) is first created. Then, a 1-nm-thick surface layer of amorphous SiO_2 is removed. The removal process leaves some dangling Si and O atoms. The dangling bonds of the surface Si and O atoms are respectively saturated with hydroxyl groups and H atoms, to yield the hydroxylated substrate model shown in Fig. 1b. The hydroxyl density is found to be in the range of 4 to 5 OH/nm^2 (also known as the Kiselev-Zhuravlev constant [23]). The bottom layer of substrate, representing a thickness of 0.2 nm, is kept fixed in order to assure the stability during MD simulations and to mimic the semi-infinite substrate. A 10-nm-long and 5-nm-wide graphene sheet is placed 2 Å from the substrate. Both the graphene sheet and the surface of the substrate are parallel to the *x*-*y* plane.

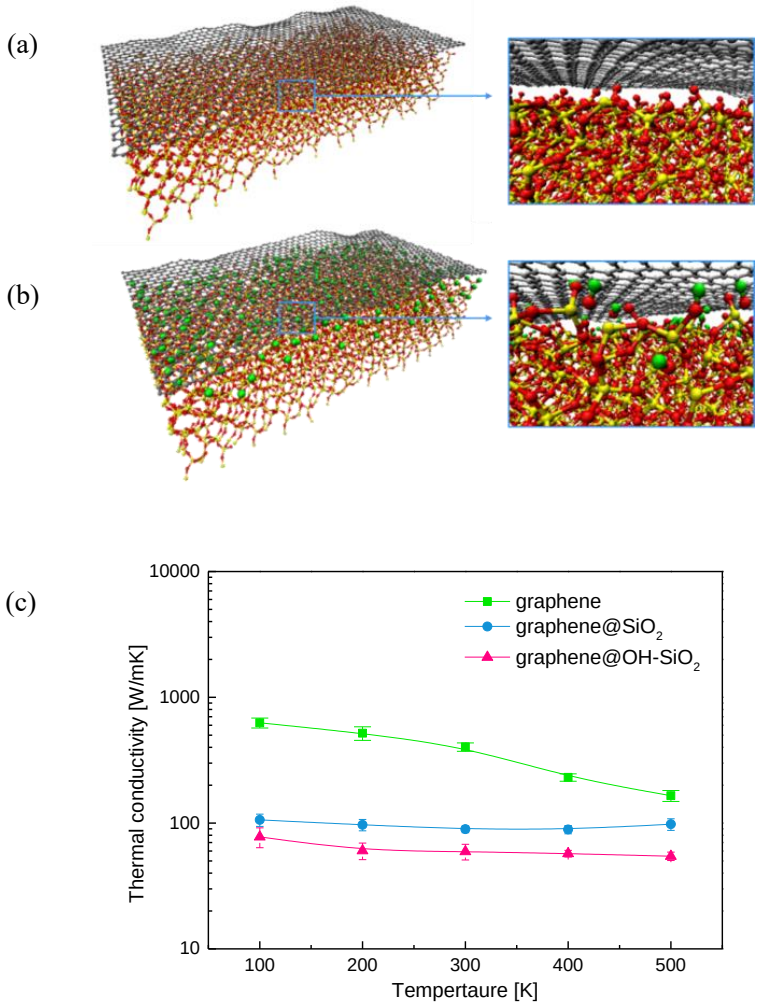

Figure 1. Geometric configuration of graphene supported on (a) the amorphous SiO_2 substrate and (b) the hydroxylated amorphous SiO_2 substrate. Gray, red, yellow and green spheres represent carbon, oxygen, silicon and hydrogen atoms, respectively. (c) Thermal conductivity of suspended graphene, and graphene supported on pristine and hydroxylated amorphous SiO_2 substrates under different temperatures.

In our study, the LAMMPS package [24] is employed to carry out MD simulations. The third-generation charge optimized many-body (COMB3) potential [25], which has been extended to a description of systems containing C, O, Si and H [20, 26], is adopted to describe the interatomic interactions in supported graphene systems. A Lennard-Jones (LJ) term included in COMB3 potential describes the van der Waals interactions. Two distinct sets of LJ parameters were used for graphene sheets supported on the bare

amorphous SiO_2 substrate and on the hydroxylated amorphous SiO_2 substrate, respectively. Both sets of parameters are taken from Ref. [20]. Using non-equilibrium MD (NEMD) simulations, we examine the thermal transport in supported graphene. The periodic boundary conditions are used in the in-plane directions (parallel to the graphene plane), while the free boundary condition is applied in the out-of-plane direction (perpendicular to the graphene plane). The time step is set as 0.5 fs. In order to establish a temperature gradient, the Nosé-Hoover thermostats [27-28] with different temperatures are attached to the two ends of the system. The thermal conductivity of supported graphene is obtained from the Fourier's Law. More details of NEMD simulations are provided in Supporting Information I. The results presented here are averaged over 5 independent simulations starting from different initial conditions, and standard deviation error bars are marked.

3. Results and discussion

3.1 Thermal conductivity

Fig. 1c shows, respectively, the thermal conductivities of suspended graphene, graphene supported on amorphous SiO_2 substrate (graphene@SiO_2) and graphene supported on hydroxylated amorphous SiO_2 substrate (graphene@HO-SiO_2) at different temperatures. As can be seen, both the thermal conductivity values of suspended and supported graphene sheets decrease with the temperature increases, which comes from the stronger anharmonic phonon-phonon scattering at higher temperature. However, the temperature dependence of thermal conductivity of supported graphene is much weaker than that of the suspended one. It indicates that the phonon transport in supported graphene is dominated by the phonon-substrate scattering rather than by the phonon-phonon scattering. In the temperature range of

100-500 K, the introduction of pristine or hydroxylated SiO_2 substrate results in a significant reduction of thermal conductivity. Additionally, we found that these two substrates have different impacts on heat transport in graphene. At 300 K, the reduction in thermal conductivity is about 77.8% for graphene@SiO_2 and 85.3% for graphene@HO-SiO_2. This result may inspire new strategies to control thermal transport properties of 2D materials through the surface functionalization of substrate, which are of great importance for the performance and reliability of 2D-material-based nanoelectronic devices.

It should be pointed out that our simulated thermal conductivity for suspended graphene is lower than that reported in recent measurements (ranging from 1500-5300 W/(m·K) [3-6]). This discrepancy can be attributed to the limitation of our simulation domain size [29-30]. However, while phonons are scattered by the boundaries of a finite simulation domain, it is apparent that the phonon-boundary scattering does not change the effect of substrate on phonon transport in graphene [13]. Like Refs. [31], [32] and [33], the changes in thermal properties due to the structural or environmental modifications can be found even when the simulation domains are relatively small. Our paper focuses more on the qualitative conclusion of relatively low thermal conductivity of graphene@HO-SiO_2 as compared to graphene@SiO_2 and the underlying mechanisms. Nevertheless, we expect that our finding of the difference between the thermal conductivity reduction of graphene@HO-SiO_2 and graphene@SiO_2 can inspire others to adopt various methods to pursue the exact thermal conductivity values of suspended and supported graphene sheets with different sizes.

3.2 Phonon spectral energy density

In order to explore the mechanisms for the effect of surface hydroxylation of substrate

on the thermal conductivity of supported graphene, we investigated the phonon spectral energy density (SED) $\Phi(\boldsymbol{\kappa}, \omega)$ [34], where $\boldsymbol{\kappa}$ is wave vector and ω is angular frequency. The following formula is used to calculate the phonon SED function $\Phi(\boldsymbol{\kappa}, \omega)$

$$\Phi\left(\boldsymbol{\kappa},\omega\right)=\frac{1}{4\pi\tau_0 N_T}\sum_{\alpha}\sum_{b}^{B} m_b\left|\int_0^{\tau_0}\sum_{n_{x,y,z}}^{N_T}\dot{u}_\alpha\begin{pmatrix}n_{x,y,z}\\ b\end{pmatrix};t\times\exp\left[i\boldsymbol{\kappa}\cdot\mathbf{r}\begin{pmatrix}n_{x,y,z}\\ 0\end{pmatrix}-i\omega t\right]\mathrm{d}t\right|^2 \qquad (1)$$

where τ_0 is the total simulation time, α is the Cartesian (x, y and z) index, b is the atom index in each SED unit cell, $n_{x,y,z}$ is the unit cell index in the simulation box, B is the number of atoms in the unit cell, N_T (=N_x·N_y·N_z) is the number of unit cells, $\dot{u}\begin{pmatrix}n_{x,y,z}\\ b\end{pmatrix},t\Big)$ is the velocity of b-th atom in the $n_{x,y,z}$-th SED unit cell at time t. $\mathbf{r}\begin{pmatrix}n_{x,y,z}\\ 0\end{pmatrix}$ is the equilibrium position of the $n_{x,y,z}$-th SED unit cell, and m_b is the mass of b-th atom. More SED calculation details are presented in Supporting Information II. The SED can predict phonon dispersion relations and lifetimes directly from MD simulations which can capture the full order anharmonic behavior of phonons, and has been used for a range of materials [35-37].

Fig. 2a illustrates the phonon dispersion relation of suspended graphene, which comprises three acoustic branches (TA, LA, ZA) and three optical branches (TO, LO, ZO). Here we focus on the ZA phonons due to twofold reasons. First, a previous study [38] has suggested that the reflection symmetry about the graphene plane leads to a selection rule that strongly restricts the participation of odd number of ZA phonons in three-phonon processes, e.g. ZA+ZA↔ZA, ZA+LA/TA↔LA/TA. This, combined with their large density of states, causes the ZA phonons to provide the dominant contribution to the graphene thermal conductivity. Second, the ZA phonons are sensitive to the out-of-plane perturbations, and hence the effect of substrate on phonon activities could be clearly extracted from the ZA branch [14, 39]. The normalized SED for

zone-center ZA phonons is particularly investigated and the results are shown in Fig. 2b. For suspended graphene, there is only one distinct peak in the spectrum relating SED to frequency, whose position corresponds to the ZA phonon with the lowest frequency allowed for the system (i.e. the cut-off frequency) [40]. Compared to the suspended graphene, a blue-shift of the ZA peak is obtained in graphene@SiO_2 and graphene@HO-SiO_2, which can be attributed to the breakdown of the selection rule due to the substrate coupling. A similar frequency shift of the ZA peak has been reported in graphene supported on amorphous SiO_2 substrate [13-14] and *h*-BN substrate [39]. The blue-shift of the ZA peak indicates that the introduction of substrate causes an increase in the cut-off frequency, which comes from the strong coupling of graphene ZA modes to the substrate modes [14, 39]. That is, the substrate acts as a high-pass filter, preventing a portion of low-frequency phonons from contributing to thermal transport. Correspondingly, the thermal conductivity of supported graphene decreases. Interestingly, the ZA phonon peak of graphene@HO-SiO_2 has a smaller blue-shift than that of graphene@SiO_2. It reveals that the surface hydroxylation of substrate helps in preserving the contribution of low-frequency phonons and is beneficial to the heat transfer in graphene, which is related to the fact that the surface hydroxylation weakens the vdW interaction between graphene and substrate [20]. However, the thermal conductivity of graphene@HO-SiO_2 is not higher than graphene@SiO_2. This observation may suggest that the heat conduction in supported graphene should not be determined solely by the low-frequency cut-off of ZA phonons. Furthermore, as shown in Fig. 2b, several new peaks appear for graphene@SiO_2 and graphene@HO-SiO_2. These peaks correspond to the out-of-plane vibration modes, which may be similar to the layer breathing mode in few-layer graphene [41]. The newly created phonon modes have small group velocities and short phonon lifetimes due to the substrate scattering

[14, 42] and thus contribute little to thermal transport.

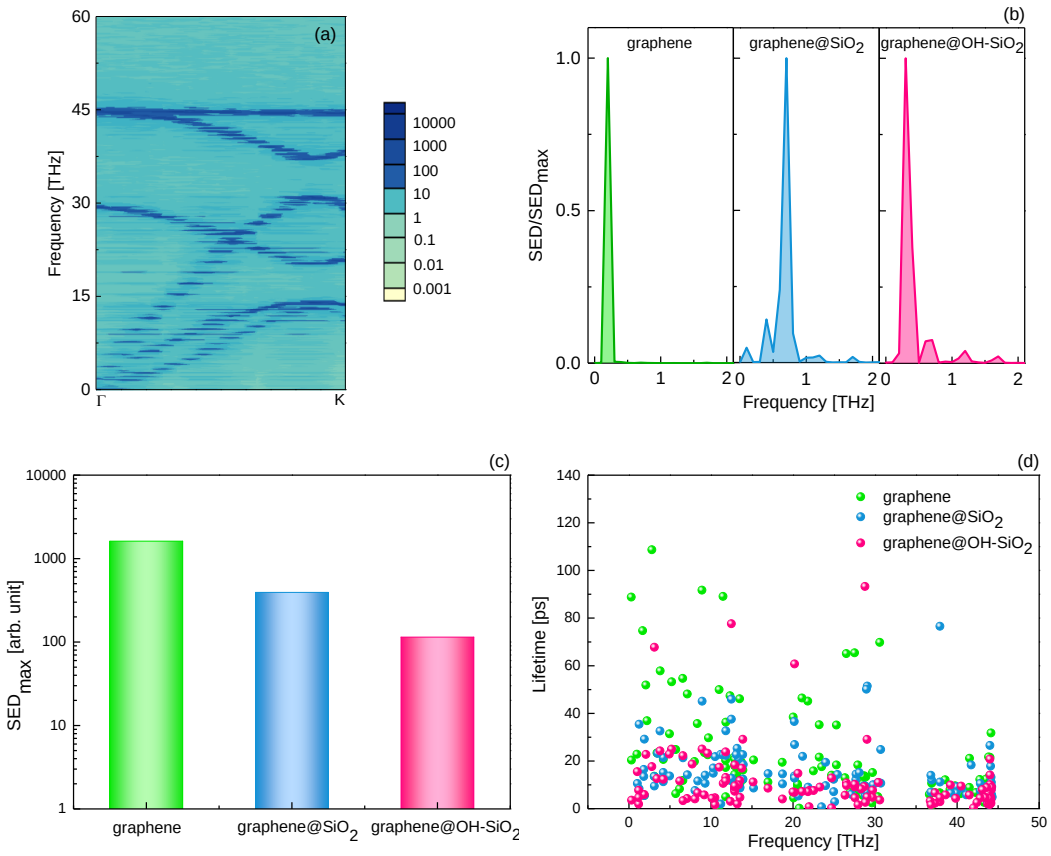

Figure 2. (a) Phonon dispersion relation of suspended graphene. (b) Normalized SED for zone-center ZA phonons in suspended and supported graphene. (c) SED intensity of the zone-center ZA peaks for suspended and supported graphene. (d) Phonon lifetimes of suspended and supported graphene.

On the other hand, the introduced substrate leads to a notable reduction in the peak intensity as shown in Fig. 2c, which implies that the ZA phonons are dramatically suppressed due to the introduction of substrate. Fig. 2c also shows that the peak intensity of graphene@HO-SiO_2 is much lower than that of graphene@SiO_2. This reveals that surface hydrogenation may strengthen the inhibitory effect of the substrate on ZA phonons, which may come from more pronounced morphological-differences in graphene@HO-SiO_2 (details in Fig. 3e). It may help to explain the relatively low thermal conductivity of graphene@HO-SiO_2.

Recently, Fugallo et al. [43] raised an interesting possibility that collective phonon

excitations, as opposed to single phonons, carry most of the heat in freestanding graphene. This result was later confirmed by additional studies [20, 44-46]. The collective phonon excitations, nicknamed relaxons, correspond to the eigenvectors of the scattering matrix in the Boltzmann equation [47]. It should be noted that SED is a frequency domain normal mode analysis method [48], which only considers single-phonon excitations as heat carriers. The effect of substrate on collective phonon excitations of graphene was not investigated in our SED analysis, but can be found in the work of France-Lanord et al. [20], which is based on a time domain normal mode analysis.

3.3 Phonon lifetime

To gain a better insight for thermal conductivity reduction of graphene@HO-SiO_2, the phonon lifetime was calculated. The expression for SED can be written as a sum (over all polarizations) of Lorentzian functions [36]

$$\Phi\left(\boldsymbol{\kappa},\omega\right)=\sum_{\nu=1}^{3B}\frac{C\left(\boldsymbol{\kappa},\nu\right)}{\left[4\pi\tau\left(\omega-\omega_0\left(\boldsymbol{\kappa},\omega\right)\right)\right]^2+1} \tag{2}$$

where τ is the phonon lifetime, $C(\boldsymbol{\kappa}, \nu)$ and $\omega_0(\boldsymbol{\kappa}, \nu)$ are the peak magnitude and frequency for the phonon branch denoted by ν. Therefore, the phonon lifetime can be evaluated by fitting the SED function with the Lorentzian function as described in Eq. (2).

Fig. 2d shows the phonon lifetimes of suspended graphene, graphene@SiO_2 and graphene@HO-SiO_2. For the suspended graphene, the frequency dependency of lifetime is not obvious, which is similar to that reported in the previous study [12]. The frequency dependence of phonon lifetimes is affected by the simulation domain size. More details of the size effect of phonon lifetimes from the SED method can be found

in Supporting Information III. When the graphene is placed on the pristine silica substrate, it is found that the phonon lifetimes are reduced throughout the full frequency range. In particular, a larger reduction in lifetimes is observed for low-frequency phonons, meaning that the substrate affects the low-frequency phonons more efficiently. By hydroxylating the substrate surface, the lifetimes decrease furtherly, meaning that phonon scattering is slightly stronger in graphene@HO-SiO_2. This may be caused by the difference in stress distribution in supported graphene. We found that the stress in graphene@HO-SiO_2 distributes more unevenly than that in graphene@SiO_2 (details in Supporting Information IV). As a result, the hydroxylated silica substrate has a stronger influence on phonon lifetimes of graphene. This lifetime difference should be the reason why graphene@HO-SiO_2 has a lower thermal conductivity than graphene@SiO_2.

3.4 Phonon participation ratio

A vibrational eigenmode analysis of phonons can further reveal the mechanisms for heat transport in graphene sheets supported on different substrates. The participation ratio for each phonon mode (p_λ) was calculated for graphene, graphene@SiO_2 and graphene@HO-SiO_2 as follows [49-50]

$$p_\lambda^{-1} = N\sum_i \left(\sum_\alpha \varepsilon_{i\alpha,\lambda}^* \varepsilon_{i\alpha,\lambda} \right)^2 \tag{3}$$

where N is the total number of atoms. $\varepsilon_{i\alpha,\lambda}$ is the i-th component of the vibrational eigenvector of the mode λ in the α-direction, with α corresponding to x, y and z. p_λ represents the extent of participation of the constituent atoms in a given phonon mode, which indicates the delocalized phonon modes with $O(1)$ and localized phonon modes with $O(1/N)$.

The calculated participation ratios are shown in Fig. 3a-c. As can be seen, the presence

of a substrate leads to the p_λ decrease. Specifically, we observe that the p_λ for low-frequency phonons decreases more seriously than that for high-frequency phonons, which is similar to the lifetime trend shown in Fig. 2d. We can figure out again that low-frequency phonons are more strongly affected by the substrate than high-frequency phonons. In addition, we find that surface hydroxylation causes a reduction in participation ratio, which is attributed to the sensitivity of graphene configuration to substrate roughness. The hydroxyl groups on the surface cause an increase in the surface roughness of SiO_2 substrate, which results in the modifications of graphene configuration. As depicted by the color maps of atomic configurations of supported graphene in Fig. 3d and 3e, morphological differences in graphene@HO-SiO_2 are more pronounced than those in graphene@SiO_2. That is, the size of morphological mismatch region (i.e. a continuous region consisting of same-colored spheres) in graphene@HO-SiO_2 is confined, and the number of morphological mismatch region becomes larger in graphene@HO-SiO_2. These morphological differences can serve as a type of disorder that localizing vibrational eigenstates [19]. Our previous study [32] has reported that the localized modes are concentrated on the joints between crests and troughs of wrinkles in graphene, which proves that the phonon localization of graphene correlates with the graphene corrugation. Since the localized phonons are less effective in transporting thermal energy than the delocalized phonons [32, 51-52], it follows that the lower thermal conductivity of graphene@HO-SiO_2 must be expected.

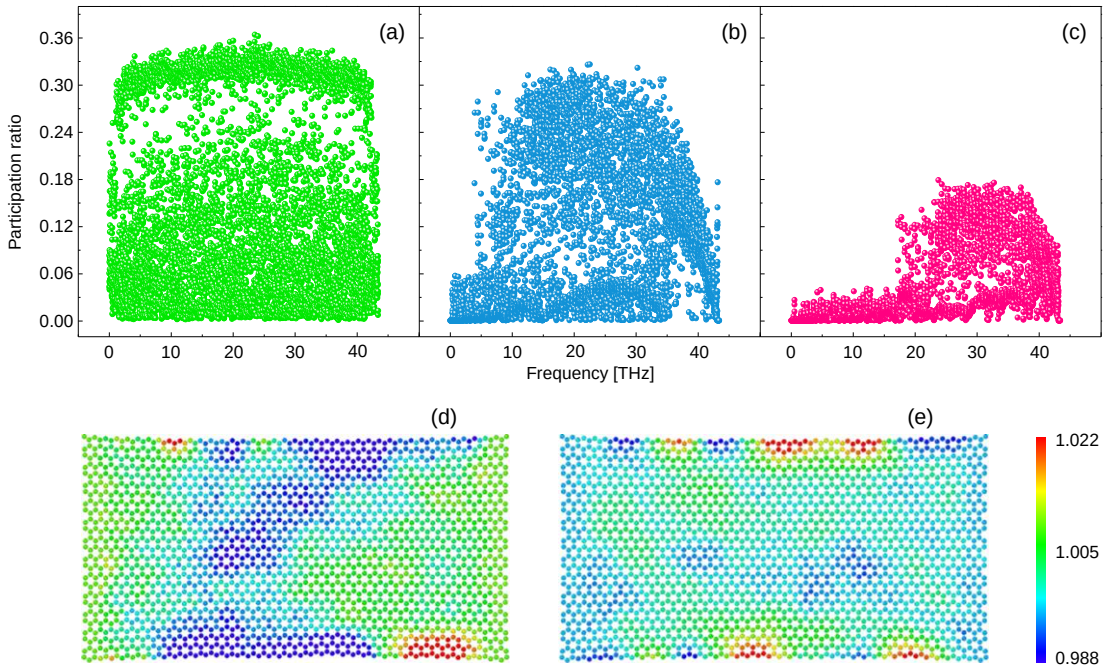

Figure 3. Phonon participation ratios of (a) suspended graphene, (b) graphene supported on amorphous SiO_2 substrate and (c) graphene supported on hydroxylated amorphous SiO_2 substrate. Atomic configurations of (d) graphene supported on amorphous SiO_2 substrate and (e) graphene supported on hydroxylated amorphous SiO_2 substrate. Different colors of spheres in (d) and (e) indicate different values of atomic coordinate in the out-of-plane direction.

4. Conclusions

Non-equilibrium molecular dynamics simulations were employed to study the influence of surface hydroxylated substrate on the thermal transport in graphene. The results demonstrate that the thermal conductivity of supported graphene is decreased by adding hydroxyl groups on the substrate surface. The SED analysis indicates that the thermal transport in the supported graphene should not be determined exclusively by the low-frequency cut-off of ZA phonons. Moreover, the hydroxyl groups cause damping of ZA phonons of graphene. The phonon lifetime, obtained by fitting the SED profile with a Lorentzian function, exhibits the lower value since the effect of phonon scattering are slightly stronger in graphene supported on hydroxylated

substrate. The phonon participation ratio spectra reveal that the surface hydroxylation also leads to the phonon localization, since more pronounced morphological-differences are induced in graphene. These findings are helpful for further utilization of graphene.

Acknowledgements

The authors are thankful for financial support from the National Natural Science Foundation of China (No. 51806064, 51741604, 51676069 and 51776066), China Postdoctoral Science Foundation Funded Project (No. 2016M600980), Hong Kong Scholars Program (No. XJ2016042), and Fundamental Research Funds for the Central Universities (No. 2018QN047 and 2015ZZD09).

Supporting Information

Calculation details for non-equilibrium molecular dynamics simulation and phonon spectral energy density; size effect of phonon lifetimes from the SED method; and stress distribution in supported graphene.

References

1. Katsnelson, M. I., Graphene: Carbon in Two Dimensions. *Mater. Today* **2007**, *10*, 20-27.

2. Shahil, K. M. F.; Balandin, A. A., Thermal Properties of Graphene and Multilayer Graphene: Applications in Thermal Interface Materials. *Solid State Commun.* **2012**, *152*, 1331-1340.

3. Balandin, A. A.; Ghosh, S.; Bao, W.; Calizo, I.; Teweldebrhan, D.; Miao, F.; Lau,

C. N., Superior Thermal Conductivity of Single-Layer Graphene. *Nano Lett.* **2008**, *8*, 902-907.

4. Chen, S.; Moore, A. L.; Cai, W.; Suk, J. W.; An, J.; Mishra, C.; Amos, C.; Magnuson, C. W.; Kang, J.; Shi, L., et al., Raman Measurements of Thermal Transport in Suspended Monolayer Graphene of Variable Sizes in Vacuum and Gaseous Environments. *ACS Nano* **2010**, *5*, 321-328.

5. Lee, J. U.; Yoon, D.; Kim, H.; Lee, S. W.; Cheong, H., Thermal Conductivity of Suspended Pristine Graphene Measured by Raman Spectroscopy. *Phys. Rev. B* **2011**, *83*, 081419.

6. Xu, X.; Pereira, L. F. C.; Wang, Y.; Wu, J.; Zhang, K.; Zhao, X.; Bae, S.; Bui, C. T.; Xie, R.; Thong, J. T. L., et al., Length-Dependent Thermal Conductivity in Suspended Single-Layer Graphene. *Nat. Commun.* **2014**, *5*, 3689.

7. Sadeghi, M. M.; Pettes, M. T.; Shi, L., Thermal Transport in Graphene. *Solid State Commun.* **2012**, *152*, 1321-1330.

8. Zhang, G.; Zhang, Y., Thermal Properties of Two-Dimensional Materials. *Chin. Phys. B* **2017**, *26*, 034401.

9. Cai, W.; Moore, A. L.; Zhu, Y.; Li, X.; Chen, S.; Shi, L.; Ruoff, R. S., Thermal Transport in Suspended and Supported Monolayer Graphene Grown by Chemical Vapor Deposition. *Nano Lett.* **2010**, *10*, 1645-1651.

10. Guo, Z.; Ding, J.; Gong, X., Substrate Effects on the Thermal Conductivity of Epitaxial Graphene Nanoribbons. *Phys. Rev. B* **2012**, *85*, 235429.

11. Seol, J. H.; Jo, I.; Moore, A. L.; Lindsay, L.; Aitken, Z. H.; Pettes, M. T.; Li, X.; Yao, Z.; Huang, R.; Broido, D., Two-Dimensional Phonon Transport in Supported Graphene. *Science* **2010**, *328*, 213-216.

12. Qiu, B.; Ruan, X., Reduction of Spectral Phonon Relaxation Times from

Suspended to Supported Graphene. *Appl. Phys. Lett.* **2012**, *100*, 193101.

13. Ong, Z. Y.; Pop, E., Effect of Substrate Modes on Thermal Transport in Supported Graphene. *Phys. Rev. B* **2011**, *84*, 075471.

14. Chen, J.; Zhang, G.; Li, B., Substrate Coupling Suppresses Size Dependence of Thermal Conductivity in Supported Graphene. *Nanoscale* **2013**, *5*, 532-536.

15. Pettes, M. T.; Jo, I.; Yao, Z.; Shi, L., Influence of Polymeric Residue on the Thermal Conductivity of Suspended Bilayer Graphene. *Nano Lett.* **2011**, *11*, 1195-1200.

16. Wang, T.; Guo, Q.; Ao, Z.; Liu, Y.; Wang, W.; Sheng, K.; Yu, B., The Tunable Bandgap of AB-Stacked Bilayer Graphene on SiO_2 with H_2O Molecule Adsorption. *Chin. Phys. Lett.* **2011**, *28*, 117302.

17. Ewing, C. S.; Bhavsar, S.; Veser, G.; McCarthy, J. J.; Johnson, J. K., Accurate Amorphous Silica Surface Models from First-Principles Thermodynamics of Surface Dehydroxylation. *Langmuir* **2014**, *30*, 5133-5141.

18. Lee, J.; Lee, N.; Lansac, Y.; Jang, Y. H., Charge Inhomogeneity of Graphene on SiO_2: Dispersion-Corrected Density Functional Theory Study on the Effect of Reactive Surface Sites. *RSC Adv.* **2014**, *4*, 37236-37243.

19. Lee, Y.; Pak, A. J.; Paek, E.; Hwang, G. S., Principal Role of Contact-Force Distribution in Determining the Thermal Conductivity of Supported Graphene. *Phys. Rev. Appl.* **2015**, *4*, 014006.

20. France-Lanord, A.; Soukiassian, P.; Glattli, C.; Wimmer, E., Thermal Transport in Supported Graphene: Substrate Effects on Collective Excitations. *Phys. Rev. Appl.* **2017**, *7*, 034030.

21. Chen, J.; Zhang, G.; Li, B., Thermal Contact Resistance across Nanoscale Silicon Dioxide and Silicon Interface. *J. Appl. Phys.* **2012**, *112*, 064319.

22. Miwa, R. H.; Orellana, W.; Fazzio, A., Carbon Nanotube Adsorbed on

Hydrogenated Si (0 0 1) Surfaces. *Appl. Surf. Sci.* **2005**, *244*, 124-128.

23. Zhuravlev, L. T., The Surface Chemistry of Amorphous Silica. Zhuravlev Model. *Colloids Surf. A* **2000**, *173*, 1-38.

24. Plimpton, S., Fast Parallel Algorithms for Short-Range Molecular Dynamics. *J. Comput. Phys.* **1995**, *117*, 1-19.

25. Liang, T.; Shan, T. R.; Cheng, Y.; Devine, B. D.; Noordhoek, M.; Li, Y.; Lu, Z.; Phillpot, S. R.; Sinnott, S. B., Classical Atomistic Simulations of Surfaces and Heterogeneous Interfaces with the Charge-Optimized Many Body (COMB) Potentials. *Mat. Sci. Eng. R* **2013**, *74*, 255-279.

26. France-Lanord, A.; Soukiassian, P.; Glattli, C.; Wimmer, E., *Ab Initio* Parameterization of a Charge Optimized Many-Body Forcefield for Si–SiO_2: Validation and Thermal Transport in Nanostructures. *J. Chem. Phys.* **2016**, *144*, 104705.

27. Nosé, S., A Unified Formulation of the Constant Temperature Molecular Dynamics Methods. *J. Chem. Phys.* **1984**, *81*, 511-519.

28. Hoover, W. G., Canonical Dynamics: Equilibrium Phase-Space Distributions. *Phys. Rev. A* **1985**, *31*, 1695.

29. Schelling, P. K.; Phillpot, S. R.; Keblinski, P., Comparison of Atomic-Level Simulation Methods for Computing Thermal Conductivity. *Phys. Rev. B* **2002**, *65*, 144306.

30. Sellan, D. P.; Landry, E. S.; Turney, J. E.; McGaughey, A. J. H.; Amon, C. H., Size Effects in Molecular Dynamics Thermal Conductivity Predictions. *Phys. Rev. B* **2010**, *81*, 214305.

31. Hu, J.; Schiffli, S.; Vallabhaneni, A.; Ruan, X.; Chen, Y., Tuning the Thermal Conductivity of Graphene Nanoribbons by Edge Passivation and Isotope Engineering: A Molecular Dynamics Study. *Appl. Phys. Lett.* **2010**, *97*, 133107.

32. Cui, L.; Du, X.; Wei, G.; Feng, Y., Thermal Conductivity of Graphene Wrinkles: A Molecular Dynamics Simulation. *J. Phys. Chem. C* **2016**, *120*, 23807-23812.

33. Hu, J.; Ruan, X.; Chen, Y., Thermal Conductivity and Thermal Rectification in Graphene Nanoribbons: A Molecular Dynamics Study. *Nano Lett.* **2009**, *9*, 2730-2735.

34. Thomas, J. A.; Turney, J. E.; Iutzi, R. M.; Amon, C. H.; McGaughey, A. J. H., Predicting Phonon Dispersion Relations and Lifetimes from the Spectral Energy Density. *Phys. Rev. B* **2010**, *81*, 081411.

35. Ding, Z.; Pei, Q.; Jiang, J.; Zhang, Y., Manipulating the Thermal Conductivity of Monolayer MoS_2 Via Lattice Defect and Strain Engineering. *J. Phys. Chem. C* **2015**, *119*, 16358-16365.

36. Li, C.; Li, G.; Zhao, H., Thermal Conductivity Variation of Graphene with Patterned Double-Side Hydrogen Doping. *J. Appl. Phys.* **2015**, *118*, 075102.

37. Honarvar, H.; Hussein, M. I., Spectral Energy Analysis of Locally Resonant Nanophononic Metamaterials by Molecular Simulations. *Phys. Rev. B* **2016**, *93*, 081412.

38. Lindsay, L.; Broido, D. A.; Mingo, N., Flexural Phonons and Thermal Transport in Graphene. *Phys. Rev. B* **2010**, *82*, 115427.

39. Zhang, Z.; Hu, S.; Chen, J.; Li, B., Hexagonal Boron Nitride: A Promising Substrate for Graphene with High Heat Dissipation. *Nanotechnology* **2017**, *28*, 225704.

40. Wei, Z.; Yang, J.; Bi, K.; Chen, Y., Mode Dependent Lattice Thermal Conductivity of Single Layer Graphene. *J. Appl. Phys.* **2014**, *116*, 153503.

41. Kong, B. D.; Paul, S.; Nardelli, M. B.; Kim, K. W., First-Principles Analysis of Lattice Thermal Conductivity in Monolayer and Bilayer Graphene. *Phys. Rev. B* **2009**, *80*, 033406.

42. Chen, L.; Kumar, S., Thermal Transport in Graphene Supported on Copper. *J. Appl. Phys.* **2012**, *112*, 043502.

43. Fugallo, G.; Cepellotti, A.; Paulatto, L.; Lazzeri, M.; Marzari, N.; Mauri, F., Thermal Conductivity of Graphene and Graphite: Collective Excitations and Mean Free Paths. *Nano Lett.* **2014**, *14*, 6109-6114.

44. Lee, S.; Broido, D.; Esfarjani, K.; Chen, G., Hydrodynamic Phonon Transport in Suspended Graphene. *Nat. Commun.* **2015**, *6*, 6290.

45. Cepellotti, A.; Fugallo, G.; Paulatto, L.; Lazzeri, M.; Mauri, F.; Marzari, N., Phonon Hydrodynamics in Two-Dimensional Materials. *Nat. Commun.* **2015**, *6*, 6400.

46. Gill-Comeau, M.; Lewis, L. J., On the Importance of Collective Excitations for Thermal Transport in Graphene. *Appl. Phys. Lett.* **2015**, *106*, 193104.

47. Cepellotti, A.; Marzari, N., Thermal Transport in Crystals as a Kinetic Theory of Relaxons. *Phys. Rev. X* **2016**, *6*, 041013.

48. Feng, T.; Ruan, X., Prediction of Spectral Phonon Mean Free Path and Thermal Conductivity with Applications to Thermoelectrics and Thermal Management: A Review. *J. Nanomater.* **2014**, *2014*.

49. Cui, L.; Zhang, Y.; Du, X.; Wei, G., Computational Study on Thermal Conductivity of Defective Carbon Nanomaterials: Carbon Nanotubes versus Graphene Nanoribbons. *J. Mater. Sci.* **2018**, *53*, 4242-4251.

50. Bodapati, A.; Schelling, P. K.; Phillpot, S. R.; Keblinski, P., Vibrations and Thermal Transport in Nanocrystalline Silicon. *Phys. Rev. B* **2006**, *74*, 245207.

51. Chen, J.; Zhang, G.; Li, B., Remarkable Reduction of Thermal Conductivity in Silicon Nanotubes. *Nano Lett.* **2010**, *10*, 3978-3983.

52. Hu, M.; Giapis, K. P.; Goicochea, J. V.; Zhang, X.; Poulikakos, D., Significant Reduction of Thermal Conductivity in Si/Ge Core-Shell Nanowires. *Nano Lett.* **2010**, *11*, 618-623.

Table of Contents Graphic